

Pseudo-Static Analysis of Soil Nailed Excavations

Gosavi Meenal · Swami Saran · Satyendra Mittal

Received: 24 August 2006 / Accepted: 30 March 2009 / Published online: 27 May 2009
© Springer Science+Business Media B.V. 2009

Abstract In this paper, a pseudo-static analysis has been presented to investigate the stability of soil nailed vertical/nearly vertical excavations. The failure surface is assumed as the arc of log-spiral passing through the toe of the excavation and intersecting the ground at right angle. The horizontal and vertical seismic forces are taken in terms of horizontal and vertical seismic coefficients. The internal failure mode of the nailed cut is considered either by pull-out or rupture or excessive bending whichever is critical. Expression for the factor of safety is derived using moment equilibrium method. Results have been arranged in tabular form considering ranges of the design parameters usually occur in practice. A typical table for the design of nailed excavation with driven nails is presented in the paper. Analytical results have been compared with the findings of model tests and reasonably good agreement has been observed.

Keywords Soil nailing · Pseudo-static analysis · Factor of safety · Parametric study · Model tests · Comparison · Good agreement

List of symbols

A_s	Area of nail = $\pi/4 d^2$
c	Cohesion acting along the surface of sliding wedge bd
C'	Is a constant and considered as $C' = 4$ for the plastic analysis (Jewell and Pedley 1990)
d	Diameter of the driven nail
f^*	Apparent coefficient of friction between nail and soil. It is obtained from pull out tests
f_y	Yield strength of steel nail
i	Number of nail, It varies from $i = 1$ to $i = N$
K_a	$\frac{1 - \sin \phi}{1 + \sin \phi}$
l_i	Length of the i th nail behind the failure wedge
l_{si}	Shear width = $\sqrt{\frac{8M_p}{\sigma_b} \times \frac{1}{d} \times \left(1 - \frac{T_i}{T_v}\right)}$
M_1	Moment of force W_1 along the center of log-spiral i.e., point 'o'
M_2	Moment of W_2 along the point 'o'
M_3	Moment of W_3 along the point 'o'
M_4	Moment of W_4 along the point 'o'
M_5	Moment of $W_1\alpha_h$ along the point 'o'
M_6	Moment of $W_2\alpha_h$ along the point 'o'
M_7	Moment of $W_3\alpha_h$ along the point 'o'
M_8	Moment of $W_4\alpha_h$ along the point 'o'
M_{Qv}	Moment of $Q (1 \pm \alpha_v)$ about the point 'o'

G. Meenal (✉) · S. Saran · S. Mittal
Department of Civil Engineering, College of Technology,
G.B. Pant University of Agriculture and Technology,
Pantnagar, Distt. UdhamSingh Nagar,
Uttarakhand 263 145, India
e-mail: meenalgulati@rediffmail.com

S. Saran
e-mail: saranfce@iit.ernet.in

S. Mittal
e-mail: smittfce@iit.ernet.in

M_{QH}	Moment of Q α_h about the point 'o'
M_C	Moment of cohesion force c about the point 'o'
M_T	Moment of nail axial force T_i of the i th nail about the point 'o'
M_{Tc}	Moment of the mobilised shear force Tc_i acting normal to the axis of nail
M_P	Fully plastic bending moment of nail varying with shape of nail
N	Total number of nails in a single column of nails
P_i	Perimeter of the i th nail (i.e., πd)
q	Applied surcharge intensity on the ground surface
Tc_i	Mobilised shear in the i th nail which acts normal to the axis of nail at its intersection with slip surface, Jewell and Pedley (1990)
T_p	Fully plastic axial force = $f_y \times A_s$
W_1	Weight of the soil wedge obd
W_2	Weight of the soil wedge oed
W_3	Weight of the soil wedge eab
W_4	Weight of the soil wedge aba'
σ_{n_i}	Normal stress at the mid depth of i th nail in the length l_i
σ_{n_i}	$\frac{\sigma_v \cos^2 \theta - \sigma_x \sin^2 \theta}{[\cos 2\theta + \sin 2\theta \tan \delta]}$
σ_y	$[\gamma(i - 0.5) S_v + q]$
σ_b	Soil bearing pressure
σ_v	$\gamma(i - 0.5) S_v$
ω	Log spiral angle

1 Introduction

Soil nailing is a method of reinforcing the soil with steel bars or other materials. The purpose is to support the tensile and shear stresses in soil and restrain its lateral displacements. The nails are either placed in drilled bore holes and grouted along their total length to form 'grouted nails', or simply driven into the ground, called as 'driven nails'. The technique helps stabilisation of both natural slopes and vertical or inclined cuts.

Many investigators (Gässler and Gudehus 1981, 1983; Shen et al. 1981; Schlosser 1982; Juran et al. 1988, 1990; Juran and Elias 1992; Raju 1996; Gupta 2003) have proposed methods for investigating the stability of vertical/nearly vertical excavations. In each method, the assumed geometry of the slip surface is based on observations in either small scale model tests

or full scale structures. The methods vary with the geometry of the assumed failure surface, the definition of the factor of safety and the forces assumed to act on the active zone. Patra and Basudhar (2001) presented an overview of experimental and theoretical studies leading to the development of various methods of analysis of soil nailed structures. The methods proposed by Raju (1996) and Gupta (2003) are based on moment equilibrium approach assuming the rupture surface as log-spiral meeting the ground at 90°. The formation of log-spiral rupture surface is supported by earlier investigators (Chen 1975; Jewell 1989; Plumelle and Schlosser 1990; Juran and Elias 1992) including the observations of Raju (1996) in his small scale model tests and trench tests.

The behaviour of soil nailed walls under dynamic loads has been studied by very few investigators. Mizuno and Chen (1984) performed seismic analysis of vertical slopes using plasticity models, and compared the results with finite element method and limit analysis methods. Sabhahit et al. (1996) presented a seismic design of nailed slopes based on pseudo-dynamic approach. Saha et al. (2002) carried out dynamic analysis of soil nailed vertical cuts using an explicit finite difference tool FLAC (Fast Lagrangian Analysis of Continua), where he considering sinusoidal harmonic horizontal shear loading only.

In this paper, a pseudo-static analysis for analysing the stability of inclined nailed cuts with driven nails is developed and presented. It is followed by the modifications in the present analysis for grouted nails.

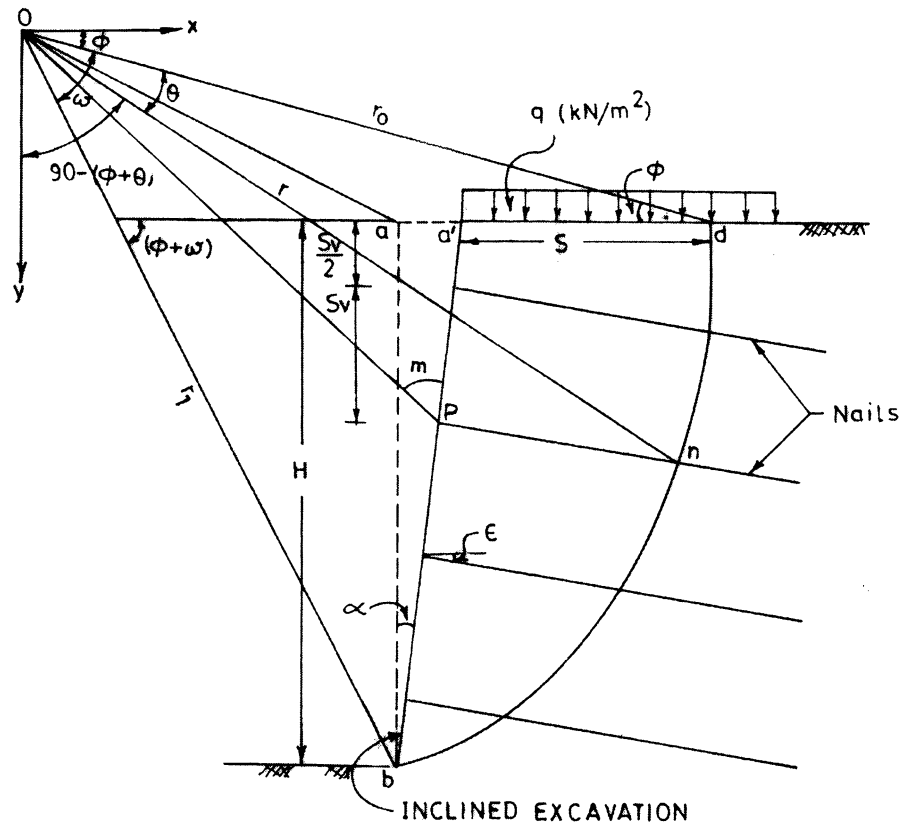
2 Analysis for Driven Nails

2.1 Assumptions

The analysis is based on the following assumptions:

1. The deformation of the soil in the active zone is sufficient to fully mobilise the shear strength of the soil over the entire failure surface.
2. The failure is along a surface defined by the arc of a log-spiral passing through the toe and intersecting the ground level at right angle. The center of the log-spiral is located on a straight line making an angle ϕ with the horizontal and passing through the point where the failure surface meets the ground as shown in Fig. 1.

Fig. 1 Geometry of rupture surface



3. The shear resistance of the nail due to nail bending stiffness is taken care by using the plastic analysis method suggested by Jewell and Pedley (1990). The shear resistance mobilized in the nail is calculated by limiting the soil bearing pressure to the safe value given by Eq. 1.

$$\sigma_b = \sigma_v \left[\frac{1 + K_a}{2} \right] \tan [\pi/2 + \phi/2] e^{(\pi/2+\phi) \tan \phi} \tag{1}$$

where, σ_b = limit bearing stress between the soil and nail, σ_v = vertical stress, ϕ = angle of internal friction of soil (degrees), and K_a = active earth pressure co-efficient.

4. Stress on the nail surface in the horizontal direction is assumed to be K_a times the normal stress in the vertical direction.

$$\sigma_x = K_a \sigma_y \tag{2}$$

5. The internal failure mode of the nailed cut is either by pull-out or rupture or excessive bending

leading to the formation of a plastic hinge in the nail whichever is critical.

6. The horizontal and vertical seismic forces are taken in the terms of horizontal and vertical seismic co-efficient denoted by α_h and α_v , respectively.

2.2 Geometry of Rupture Surface

Figure 1 shows an inclined nailed cut of height H with face $a'b'$. Here, α is the inclination of cut with vertical (angle aba'). Nails are provided at an inclination ϵ with horizontal at a vertical spacing S_v . N represents the number of nails per column which will be equal to (H/S_v) ; Fig. 1). The rupture surface is taken as log-spiral having equation as:

$$r_1 = r_0 e^{\omega \tan \phi} = ob \tag{3}$$

where, r_0 = od , i.e., initial radius of log-spiral, r_1 = ob , i.e., radius of log spiral at an angle ω measured from od , and ω = log-spiral angle.

The log-spiral strikes the ground at 90° at a distance 's' from the point a'. The center (o) of log-spiral lies on the line od which makes angle φ with the horizontal. Since, ob = oe + eb

$$r_o e^{\omega \tan \phi} = \frac{r_o \sin \phi}{\sin(\phi + \omega)} + H \operatorname{cosec}(\phi + \omega) \tag{4}$$

Therefore,

$$r_o = \frac{H \operatorname{cosec}(\phi + \omega)}{e^{\omega \tan \phi} - \frac{\sin \phi}{\sin(\phi + \omega)}} \tag{5}$$

$$\text{Or } r_o = od = H \cdot x \tag{6}$$

where, x is a constant which is a function of φ and ω and is represented as

$$x = \frac{\operatorname{cosec}(\phi + \omega)}{e^{\omega \tan \phi} - \frac{\sin \phi}{\sin(\phi + \omega)}} \tag{7}$$

$$s = a'd = ed - ea - aa'$$

$$\text{Or, } s = \frac{r_o \sin \omega}{\sin(\phi + \omega)} - H \cot(\phi + \omega) - H \tan \alpha \tag{8}$$

$$\text{Let } s = Hy \tag{9}$$

$$\text{Hence, } y = \frac{x \sin \omega}{\sin(\phi + \omega)} - \cot(\phi + \omega) - \tan \alpha \tag{10}$$

$$le_i = L - pn \text{ (Fig. 2)} \tag{11}$$

where, le_i = Length of nail behind failure surface, L = Length of nail used

$$pn = \frac{op \cdot \cos(m + \phi + \omega_i)}{\sin(\phi + \omega_i - \epsilon)} \tag{12}$$

$$l_i = on \cdot \sin(\phi + \omega_i - \epsilon) = r_o \cdot e^{\omega_i \tan \phi} \sin(\phi + \omega_i - \epsilon) \tag{13}$$

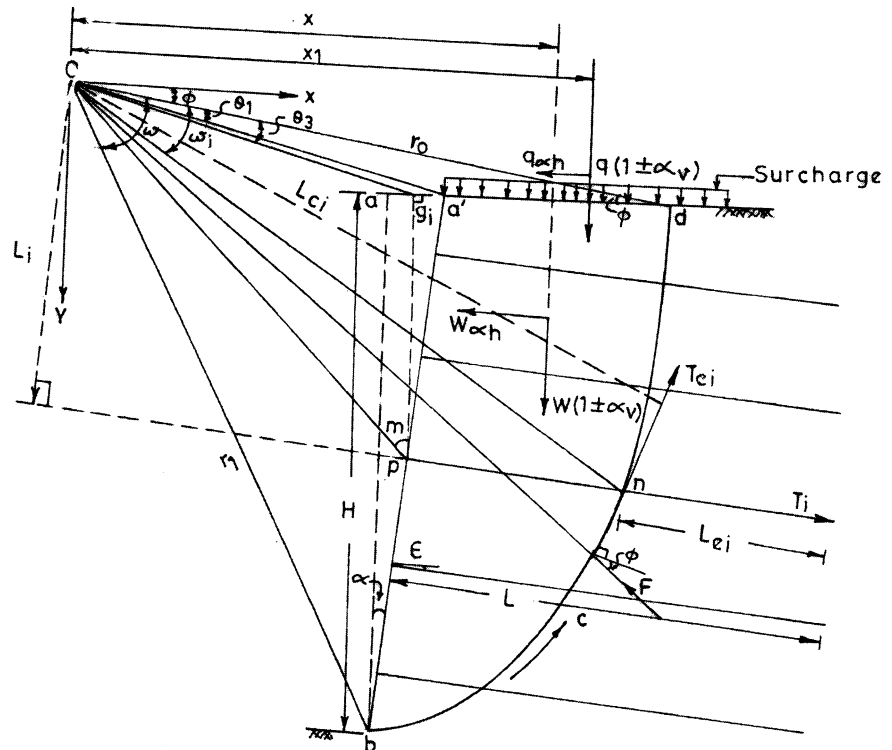
$$lc_i = on \cdot \cos \phi \tag{14}$$

$$\text{Where, } on = r_i = r_o e^{\omega_i \tan \phi} \tag{15}$$

2.3 Forces Acting on Sliding Wedge

The forces acting on the sliding wedge bounded by the logarithmic spiral arc are shown in Fig. 2, and defined as below:

Fig. 2 Forces acting on the wedge a'bd



1. $W(1 \pm \alpha_v)$, the weight of the soil wedge a'bd along with vertical seismic force. It acts at the center of gravity (c.g.) of the wedge a'bd in the vertical direction.
2. $W\alpha_h$, the horizontal seismic force acting at the c.g. of wedge.
3. $Q(1 \pm \alpha_v)$, the force due to surcharge intensity q on a'd alongwith vertical seismic force acting on it; $Q = qa'd$.
4. $Q\alpha_h$, the horizontal seismic force on surcharge.
5. F , the reaction along the surface of sliding bd, acting at an angle ϕ to the normal of log spiral bd and passes through the centre of log-spiral (o).
6. C , the force due to cohesion acting along the surface of sliding wedge bd.
7. T_i , the tensile or pull out capacity, (whichever is smaller) of the i th nail.
8. Tc_i , the maximum shear resistance mobilised in the i th nail due to bending stiffness.

The procedure of computation of various forces acting on the sliding wedge, resisting and driving moments is presented elsewhere (Saran et al. 2005; Gosavi 2006). In this paper these forces and their moments about centre of log-spiral 'o', are summarized in Table 1 using Figs. 3 and 4 in addition to Figs. 1 and 2. The expressions given in column no. 4 are obtained by multiplying the expressions given in cols. (2) and (3) and substituting the values of r_1, r_0, od, ed, aa' etc. from the Sect. 2.2. The various terms used in various expressions are explained in "List of Symbols".

2.4 Equation of Factor of Safety

The equation of Factor of Safety (FOS) is defined as:

$$FOS = \frac{\sum \text{resisting moments}}{\sum \text{driving moments}}$$

Therefore,

$$FOS = \frac{M_T + M_{Tc} + Mc}{M_{WV} + M_{WH} + M_{QV} + M_{QH}} \tag{16}$$

where, $M_{WV} = (1 \pm \alpha_v) [M_1 - M_2 - M_3 - M_4]$, $M_{WH} = (M_5 - M_6 - M_7 - M_8)$. α_h , $M_{QV} =$ moment of Q . $(1 \pm \alpha_v)$ about the point 'o', $M_{QH} =$ moment of Q . α_h about the point 'o'.

It may be seen that the expression of FOS depends on (1) soil properties: c, γ , and ϕ , (2) nail properties:

d, ε , and f_y , (3) excavation parameters: H and α , (4) co-efficient of friction between nails and soil, f^* , and (5) log-spiral angle ω . For a set of given values of $c, \phi, d, L/H, \varepsilon, f_y, H, \alpha_h$, and f^* , the FOS was computed varying log-spiral angle ω . A typical plot showing the variation of FOS with ω is shown in Fig. 5. Minimum value of FOS obtained from such plot is considered for design.

2.5 Results

For the design of nailed excavations, Tables have been prepared considering the following ranges of parameters:

H (m)	6, 8, 10, 12
ϕ ($^\circ$)	25, 30 and 35
α_h	0.0, 0.05, 0.1 and 0.15; $\alpha_v = \alpha_{h/2}$
γ	Unit weight of soil = 16.5 kN/m ³
c (kN/m ²)	0, 10, 20
q (kN/m ²)	0, 80, 120
d (mm)	25
L/H	0.8
f^*	0.5

A large number of results were analysed varying $d, L/H$ ratio and f^* , and it was found that the FOS may be obtained using following correlations, for other values of $d, L/H$, and f^* without sacrificing the accuracy:

$$(FOS) \left\{ \begin{matrix} d = x \\ L/H = x1 \\ f^* = x2 \end{matrix} \right\} = (FOS) \left\{ \begin{matrix} d = 25 \\ L/H = 0.8 \\ f^* = 0.5 \end{matrix} \right\} \times \frac{x}{25} \times \frac{x1}{0.8} \times \frac{x2}{0.5} \tag{17}$$

where, $(FOS) \left\{ \begin{matrix} d = x \\ L/H = x1 \\ f^* = x2 \end{matrix} \right\} =$ FOS corresponding to nail diameter = x mm, $L/H = x1$ and $f^* = x2$,

$(FOS) \left\{ \begin{matrix} d = 25 \\ L/H = 0.8 \\ f^* = 0.5 \end{matrix} \right\} =$ FOS corresponding to nail diameter $d = 25$ mm, $L/H = 0.8$ and $f^* = 0.5$.

Table 1 Forces and moments

Sl. no.	Force	Lever arm w.r.t. point 'o'	Moment about point 'o'
(1)	(2)	(3)	(4)
1	$W_1 = \int_0^{\omega} \int_{\frac{1}{2}}^1 r r d\theta(\downarrow)$ (Fig. 3)	$\frac{2}{3} r \cos(\phi + \theta)$	$M_1 = \frac{\gamma H^3 x^3}{3(1+9 \tan^2 \phi)} \left[e^{3\omega \tan \phi} \{3 \tan \phi \cos(\phi + \omega) + \sin(\phi + \omega)\} - 4 \sin \phi \right]$ (clockwise)
2	$W_2 = \int_{\frac{1}{2}}^1 \gamma r \text{ed} \text{od} \sin \phi(\downarrow)$ (Fig. 4)	$\frac{2}{3} \omega r \cos(\phi + \delta')$	$M_2 = \frac{1}{12} \gamma H^3 x^3 \frac{\sin^3 \omega}{\sin^3(\phi + \omega)} \frac{\sin^2 \phi \cos(\phi + \delta')}{\sin^2 \delta'}$ (clockwise)
3	$W_3 = \frac{1}{2} \gamma \text{ea} \text{ab}(\downarrow)$ (Fig. 1)	$\text{od} \cos \phi - s - a a' - \frac{2}{3} a a'$	$M_3 = \frac{1}{2} \gamma H^2 \cot(\phi + \omega) \left[x \cos \phi - y - \tan \alpha - \frac{\cot(\phi + \omega)}{3} \right]$ (clockwise)
4	$W_4 = \frac{1}{2} \gamma \text{ab} \text{aa}'(\downarrow)$ (Fig. 1)	$\text{od} \cos \phi - s - \frac{2}{3} a a'$	$M_4 = \frac{1}{2} \gamma H^3 \tan \alpha \left[x \cos \phi - y - \frac{2 \tan \alpha}{3} \right]$ (clockwise)
5	$W_1 \alpha_h = \int_0^{\omega} \int_{\frac{1}{2}}^1 \gamma r r d\theta \alpha_h(\leftarrow)$ (Fig. 3)	$\frac{2}{3} \gamma r \sin(\phi + \theta)$	$M_5 = \frac{\gamma H^3 x^3}{3(1+9 \tan^2 \phi)} \left[e^{3\omega \tan \phi} \{3 \tan \phi \sin(\phi + \omega) - \cos(\phi + \omega)\} - 3 \tan \phi \sin \phi + \cos \phi \right] \cdot \alpha_h$ (clockwise)
6	$W_2 \alpha_h = \int_{\frac{1}{2}}^1 \gamma \text{ed} \text{od} \sin \phi \alpha_h(\leftarrow)$ (Fig. 4)	$\frac{2}{3} \omega r \sin(\phi + \delta')$	$M_6 = \frac{1}{12} \gamma H^3 x^3 \frac{\sin^3 \omega}{\sin^3(\phi + \omega)} \frac{\sin^2 \phi}{\sin^2 \delta'}$ (clockwise)
7	$W_3 \alpha_h = \frac{1}{2} \gamma \text{ea} \text{ab} \alpha_h(\leftarrow)$ (Fig. 1)	$\left[\text{od} \sin \phi + \frac{a b'}{3} \right]$	$M_7 = \frac{1}{2} \gamma H^2 \cot(\phi + \omega) \left[x \sin \phi + \frac{1}{3} \right] \alpha_h$ (clockwise)
8	$W_4 \alpha_h = \frac{1}{2} \gamma \text{ab} \text{aa}' \alpha_h(\leftarrow)$ (Fig. 1)	$\left[\text{od} \sin \phi + \frac{a'}{3} \right]$	$M_8 = \frac{1}{2} \gamma H^2 \tan \alpha \left[x \sin \phi + \frac{1}{3} \right] \alpha_h$ (clockwise)
9	$q a/d(1 \pm \alpha_v) = Q(1 \pm \alpha_v)(\downarrow)$ (Fig. 1)	$\left[\text{od} \cos \phi - \frac{a d'}{2} \right]$	$M_{QV} = q H^2 y^q a' d' \alpha_h$ (clockwise)
10	$q a/d \alpha_h = Q \alpha_h(\leftarrow)$ (Fig. 1)	$\text{od} \sin \phi$	$M_{QH} = q H^2 x y \sin \phi \alpha_h$ (clockwise)
11	$C = \int_0^{\omega} c r d\theta(\rightarrow)$ (Fig. 3)	r	$M_C = \int_0^{\omega} \int_{\frac{1}{2}}^1 c r r d\theta = \frac{c}{2 \tan \phi} [r_1^2 - r_0^2]$ (anticlockwise)
12	Axial nail force T_i lesser of $(\rightarrow)_{f_s A_s}$ OR $T_i = \frac{f_s A_s}{S_h}$	$l_i = r_0 e^{\omega_i \tan \phi} \cdot \sin(\phi + \omega_i - \varepsilon)$	$M_T = \sum_{i=1}^{i=N} T_i l_i = \sigma_n \cdot f \cdot P_i l_i / S_h \cdot r_0 e^{\omega_i \tan \phi} \sin(\phi + \omega_i - \varepsilon)$ OR $= \frac{f_s A_s}{S_h} r_0 e^{\omega_i \tan \phi} \sin(\phi + \omega_i - \varepsilon)$ (anticlockwise)
13	Mobilised shear in the i th nail according to Jewell and Pedley (1990) $T_{C_i} = \frac{C M_p}{l_i S_h} \left[1 - \left(\frac{T_i}{T_p} \right) \right] (\rightarrow)$	$l_{C_i} = \text{on} \cos \phi$	$M_{TC} = \sum_{i=1}^{i=N} T_{C_i} l_{C_i} = \frac{C M_p}{l_{C_i} S_h} \left[1 - \left(\frac{T_i}{T_p} \right) \right] r_0 e^{\omega_i \tan \phi} \cos \phi$ (anticlockwise)

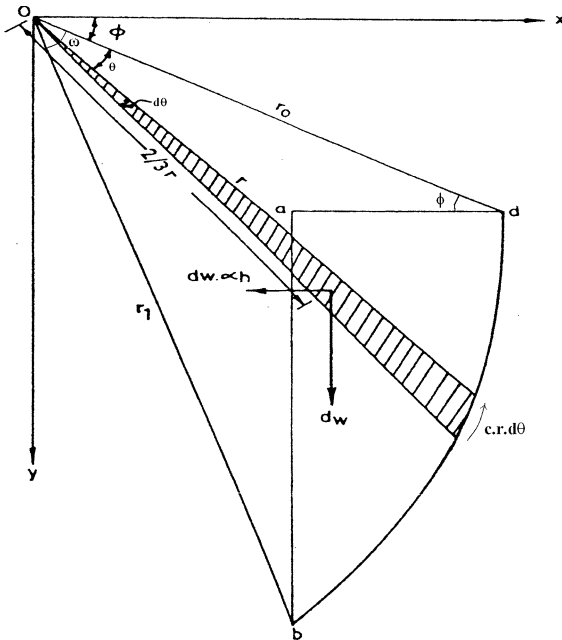


Fig. 3 Illustrating the procedure for getting moment of forces $W_1(1 \pm \alpha_v)$, $W_1 \cdot \alpha_h$ and c

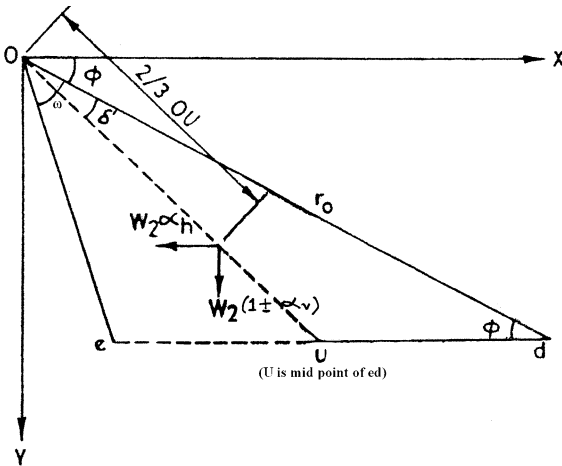


Fig. 4 Illustrating the procedure of getting moment of forces $W_2(1 \pm \alpha_v)$ and $W_2 \cdot \alpha_h$

The maximum error in the estimation of FOS using correlation 17 with respect to FOS obtained using computer program was $\pm 8\%$. Tables have been prepared for obtaining the values of $(FOS)_d = 25$ mm, $L/H = 0.8$, $f^* = 0.5$. All the 12 tables for the above mentioned data are given elsewhere (Gosavi 2006). A typical Table 2 for $\phi = 30^\circ$ and $H = 10$ m is presented here for illustration.

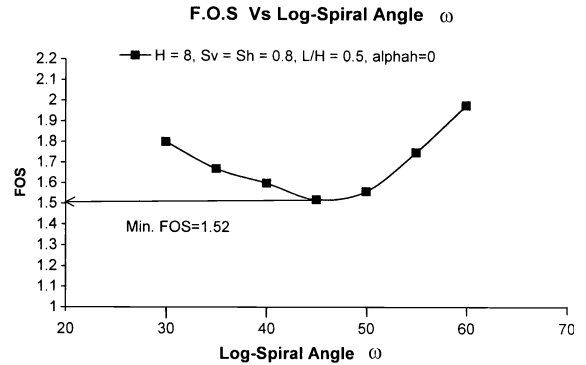


Fig. 5 Typical plot for FOS versus log-spiral angle (ω)

3 Analysis for Grouted Nails

In case grouted nails were used for stabilizing the cuts, then the certain changes are required to be made in the analysis presented in Para 2.0. Let ‘D’ be the diameter of the grouted nail (grout hole diameter).

- For the calculation of the nail axial force with the pull-out resistance criteria, perimeter of the grouted nail is calculated as:

$$P_i = \pi \cdot D$$

- The value of apparent coefficient of friction, f^* for grouted nail is to be considered in between grout and soil interface.
- For the calculation of the nail axial force with the nail breakage strength criteria, and for the calculation of fully plastic axial force in nail, i.e., T_p , area of the grouted nail is calculated as:

$$A_s = \pi/4 \cdot d^2$$

- Shear width l_{si} , is calculated for the grouted nail as:

$$l_{si} = \text{shear width} = \sqrt{\frac{8M_p}{\sigma_b} \times \frac{1}{D} \times \left(1 - \frac{T_i}{T_p}\right)}$$

Apart from the mentioned changes in the above listed equations, the analysis for the stability of inclined nailed cuts with grouted nails remains same as that for driven nails. Due to the apparently complex geometry of the log-spiral, the minimum value of FOS was determined using computer program developed during this research work in C++ language. This program can be used for the design of nailed excavation by using driven nails as

Table 2 Parametric study for $H = 10\text{ m}$, $\phi = 30^\circ$, $\gamma = 16.5\text{ kN/m}^3$, $N = H/S_v$, $L/H = 0.8$, $d = 25\text{ mm}$, $\varepsilon = 0^\circ$, $\alpha_x = \alpha_H/2$, $f_y = 4.15 \times 10^5\text{ kPa}$

α_h	α	FOS	N		N		N		N		N		N						
			$c = 0$	$q = 0$	$c = 20\text{ kPa}$	$q = 0$	$c = 10\text{ kPa}$	$q = 80\text{ kPa}$	$c = 20\text{ kPa}$	$q = 80\text{ kPa}$	$c = 0$	$q = 120\text{ kPa}$	$c = 10\text{ kPa}$	$q = 120\text{ kPa}$	$c = 20\text{ kPa}$	$q = 120\text{ kPa}$			
0	0	14	1.71	12	1.68	9	1.55	14	1.53	13	1.57	12	1.62	15	1.70	14	1.69	12	1.51
0	0	15	1.96	13	1.90	10	1.72	15	1.76	14	1.78	13	1.82	16	1.93	15	1.91	13	1.70
0	0	16	2.23	14	2.14	11	1.90	16	1.99	15	2.01	14	2.03	17	2.18	16	2.14	14	1.90
0	0	17	2.52	15	2.39	12	2.10	17	2.25	16	2.25	15	2.26	18	2.44	17	2.39	15	2.12
0	5	12	1.55	10	1.56	8	1.64	13	1.62	12	1.67	10	1.53	13	1.57	12	1.58	11	1.60
0	5	13	1.81	11	1.78	9	1.83	14	1.88	13	1.91	11	1.73	14	1.82	13	1.81	12	1.82
0	5	14	2.10	12	2.03	10	2.03	15	2.16	14	2.17	12	1.96	15	2.09	14	2.06	13	2.05
0	5	15	2.41	13	2.30	11	2.26	16	2.45	15	2.45	13	2.20	16	2.37	15	2.33	14	2.30
0	10	11	1.58	9	1.61	6	1.55	11	1.41	10	1.50	9	1.60	12	1.62	11	1.64	10	1.67
0	10	12	1.88	10	1.86	7	1.73	12	1.68	11	1.74	10	1.82	13	1.90	12	1.90	11	1.91
0	10	13	2.21	11	2.13	8	1.93	13	1.97	12	2.01	11	2.07	14	2.20	13	2.18	12	2.17
0	10	14	2.56	12	2.43	9	2.15	14	2.28	13	2.30	12	2.34	15	2.52	14	2.48	13	2.45
0	15	10	1.58	8	1.64	5	1.63	10	1.40	10	1.79	8	1.64	10	1.35	9	1.41	8	1.49
0	15	11	1.91	9	1.91	6	1.81	11	1.69	11	2.08	9	1.89	11	1.63	10	1.67	9	1.72
0	15	12	2.28	10	2.22	7	2.02	12	2.02	12	2.40	10	2.16	12	1.93	11	1.95	10	1.98
0	15	13	2.67	11	2.55	8	2.26	13	2.36	13	2.75	11	2.45	13	2.27	12	2.26	11	2.26
0.05	0	14	1.54	12	1.53	10	1.56	15	1.59	14	1.63	13	1.66	15	1.54	14	1.55	13	1.55
0.05	0	15	1.77	13	1.72	11	1.73	16	1.81	15	1.83	14	1.86	16	1.75	15	1.75	14	1.74
0.05	0	16	2.01	14	1.93	12	1.91	17	2.04	16	2.05	15	2.06	17	1.98	16	1.96	15	1.94
0.05	0	17	2.27	15	2.16	13	2.11	18	2.28	17	2.28	16	2.28	18	2.22	17	2.18	16	2.15
0.05	5	13	1.62	11	1.60	9	1.65	14	1.69	12	1.52	11	1.58	14	1.64	12	1.71	12	1.66
0.05	5	14	1.88	12	1.82	10	1.84	15	1.94	13	1.73	12	1.78	15	1.88	13	1.96	13	1.87
0.05	5	15	2.15	13	2.06	11	2.04	16	2.21	14	1.97	13	2.00	16	2.14	14	2.23	14	2.09
0.05	5	16	2.44	14	2.32	12	2.26	17	2.49	15	2.21	14	2.23	17	2.41	15	2.52	15	2.34
0.05	10	12	1.66	10	1.66	7	1.55	12	1.50	11	1.57	10	1.65	13	1.70	12	1.71	10	1.51
0.05	10	13	1.95	11	1.90	8	1.73	13	1.75	12	1.81	11	1.87	14	1.96	13	1.96	11	1.73
0.05	10	14	2.26	12	2.17	9	1.93	14	2.03	13	2.07	12	2.11	15	2.25	14	2.23	12	1.96
0.05	10	15	2.59	13	2.45	10	2.15	15	2.33	14	2.34	13	2.37	16	2.56	15	2.52	13	2.21
0.05	15	10	1.38	9	1.69	6	1.61	11	1.49	10	1.59	9	1.69	11	1.44	10	1.49	9	1.55
0.05	15	11	1.67	10	1.95	7	1.80	12	1.78	11	1.85	10	1.93	12	1.71	11	1.74	10	1.78
0.05	15	12	1.99	11	2.24	8	2.01	13	2.08	12	2.13	11	2.19	13	2.00	12	2.01	11	2.03
0.05	15	13	2.33	12	2.56	9	2.25	14	2.41	13	2.44	12	2.48	14	2.32	13	2.31	12	2.30
0.1	0	15	1.60	13	1.57	11	1.58	16	1.64	15	1.67	13	1.53	16	1.60	15	1.60	14	1.60

Table 2 continued

α_h	α	FOS	N		N		N		N		N		N		N				
			$c = 0, q = 0$	$c = 20 \text{ kPa}, q = 0$	$c = 0, q = 80 \text{ kPa}$	$c = 10 \text{ kPa}, q = 80 \text{ kPa}$	$c = 20 \text{ kPa}, q = 80 \text{ kPa}$	$c = 0, q = 120 \text{ kPa}$	$c = 10 \text{ kPa}, q = 120 \text{ kPa}$	$c = 20 \text{ kPa}, q = 120 \text{ kPa}$	$c = 0, q = 120 \text{ kPa}$	$c = 10 \text{ kPa}, q = 120 \text{ kPa}$	$c = 20 \text{ kPa}, q = 120 \text{ kPa}$						
0.1	0	16	1.82	14	1.76	12	1.75	17	1.85	16	1.87	14	1.70	17	1.80	16	1.79	15	1.78
0.1	0	17	2.05	15	1.96	13	1.93	18	2.08	17	2.08	15	1.89	18	2.02	17	1.99	16	1.98
0.1	0	18	2.29	16	2.18	14	2.12	19	2.31	18	2.30	16	2.09	19	2.24	18	2.21	17	2.18
0.1	5	14	1.68	12	1.65	9	1.50	14	1.53	13	1.58	12	1.63	15	1.70	14	1.70	12	1.52
0.1	5	15	1.93	13	1.86	10	1.67	15	1.75	14	1.79	13	1.82	16	1.93	15	1.92	13	1.71
0.1	5	16	2.19	14	2.09	11	1.85	16	1.99	15	2.01	14	2.03	17	2.18	16	2.15	14	1.91
0.1	5	17	2.47	15	2.34	12	2.05	17	2.24	16	2.25	15	2.26	18	2.44	17	2.40	15	2.13
0.1	10	12	1.47	11	1.70	8	1.56	13	1.57	12	1.63	11	1.69	13	1.52	12	1.55	11	1.57
0.1	10	13	1.73	12	1.94	9	1.74	14	1.82	13	1.86	12	1.91	14	1.76	13	1.77	12	1.78
0.1	10	14	2.00	13	2.19	10	1.94	15	2.08	14	2.11	13	2.14	15	2.02	14	2.01	13	2.01
0.1	10	15	2.30	14	2.47	11	2.15	16	2.37	15	2.38	14	2.40	16	2.29	15	2.27	14	2.25
0.1	15	11	1.47	9	1.50	7	1.61	12	1.57	11	1.66	9	1.53	12	1.52	11	1.56	10	1.61
0.1	15	12	1.75	10	1.74	8	1.80	13	1.84	12	1.91	10	1.74	13	1.78	12	1.80	11	1.83
0.1	15	13	2.05	11	1.99	9	2.01	14	2.14	13	2.18	11	1.97	14	2.06	13	2.07	12	2.08
0.1	15	14	2.37	12	2.27	10	2.24	15	2.45	14	2.47	12	2.23	15	2.36	14	2.35	13	2.34
0.15	0	16	1.64	14	1.60	12	1.60	17	1.69	15	1.53	14	1.57	17	1.64	16	1.64	15	1.64
0.15	0	17	1.85	15	1.79	13	1.76	18	1.89	16	1.72	15	1.74	18	1.83	17	1.83	16	1.82
0.15	0	18	2.07	16	1.99	14	1.94	19	2.10	17	1.91	16	1.92	19	2.04	18	2.02	17	2.01
0.15	0	19	2.31	17	2.20	15	2.13	20	2.32	18	2.11	17	2.12	20	2.26	19	2.23	18	2.20
0.15	5	14	1.51	13	1.69	10	1.52	15	1.58	14	1.63	13	1.67	15	1.53	14	1.55	13	1.57
0.15	5	15	1.73	14	1.90	11	1.69	16	1.80	15	1.83	14	1.86	16	1.74	15	1.75	14	1.75
0.15	5	16	1.97	15	2.12	12	1.87	17	2.02	16	2.05	15	2.07	17	1.97	16	1.96	15	1.95
0.15	5	17	2.22	16	2.36	13	2.06	18	2.27	17	2.28	16	2.28	18	2.20	17	2.18	16	2.16
0.15	10	13	1.54	11	1.53	9	1.58	14	1.63	13	1.68	11	1.55	14	1.58	13	1.60	12	1.63
0.15	10	14	1.78	12	1.74	10	1.75	15	1.86	14	1.91	12	1.74	15	1.81	14	1.82	13	1.83
0.15	10	15	2.05	13	1.97	11	1.95	16	2.12	15	2.15	13	1.95	16	2.05	15	2.05	14	2.05
0.15	10	16	2.33	14	2.22	12	2.16	17	2.39	16	2.40	14	2.18	17	2.32	16	2.30	15	2.28
0.15	15	12	1.54	10	1.55	8	1.62	13	1.64	12	1.71	10	1.58	13	1.58	12	1.62	11	1.66
0.15	15	13	1.81	11	1.78	9	1.81	14	1.90	13	1.96	11	1.79	14	1.83	13	1.86	12	1.88
0.15	15	14	2.09	12	2.02	10	2.02	15	2.17	14	2.22	12	2.01	15	2.10	14	2.11	13	2.12
0.15	15	15	2.40	13	2.29	11	2.24	16	2.47	15	2.50	13	2.26	16	2.38	15	2.38	14	2.37

well as grouted nails. Details about the computer program are given elsewhere (Gosavi et al. 2006). For the design of excavations stabilized with driven nails, results presented in tables may be used. In the next section, an example has been given for illustration. However, for exact design and for grouted nails, software package developed in the study may be used.

4 Illustrative Example

Design a nail cut inclined at 10° with vertical, 10 m high carrying 120 kPa surcharge. The soil properties are $c = 20$ kPa, $\gamma = 16.5$ kN/m³, $\phi = 30^\circ$. The wall has to be designed considering the effect of seismicity (i.e., $\alpha_h = 0.05$).

Adopt nails of diameter ($d = 32$ mm, $f_y = 4.15 \times 10^5$ kPa, $L/H = 0.7$, and $f^* = 0.55$. From Table 2, for $\phi = 30^\circ$, $H = 10$ m, $\alpha = 10^\circ$, $\alpha_h = 0.05$, $d = 25$ mm, $L/H = 0.8$, $f^* = 0.5$, $f_y = 4.15 \times 10^5$ kPa, $c = 20$ kPa, and $q = 120$ kPa, we get FOS as 1.51 for $N = 10$ (i.e., $S_v = S_h = 1.0$ m).

Therefore, from Eq. (17),

$$(\text{FOS}) \left\{ \begin{array}{l} d = 32\text{mm} \\ L/H = 0.7 \\ f^* = 0.55 \end{array} \right\} = 1.51 \times \frac{32}{25} \times \frac{0.7}{0.8} \times \frac{0.55}{0.5} = 1.86$$

Therefore, the value of FOS for $\phi = 30^\circ$, $H = 10$ m, $\alpha = 10^\circ$, $\alpha_h = 0.05$, $d = 32$ mm, $L/H = 0.7$, $f^* = 0.55$, $f_y = 4.15 \times 10^5$ kPa, $c = 20$ kPa, and $q = 120$ kPa is 1.86. The value of FOS of the nailed cut considering all above said parameters found out by using a computer program developed during this research work is 1.89. The difference in the value of FOS calculated by correlation equations and the computer program is only 2%.

5 Experimental Program

5.1 General

To validate the analysis, model tests were performed. Studies have been done on two model nailed cuts, each of 2.0 m high. In these model tests firstly stable

and safe vertical nailed cuts ($\alpha = 0$, $\text{FOS} \gg 1.0$) were designed using the analysis developed in this study. Then surcharge load was applied on these nailed cuts gradually and the surcharge intensity at which the stable nailed cut failed was recorded. For the failure surcharge intensities, the factor of safety of the designed nailed cuts were again obtained from the present analysis.

5.2 Soil and Nails Used

The soil used in the study was poorly graded sand Fig. 6 (SP, $D_{10} = 0.16$ mm, $C_u = 5$, $G = 2.54$, $e_{\min} = 0.45$, and $e_{\max} = 0.79$). The soil was placed in model excavations at a unit weight of 16.5 kN/m³. The value of ϕ at this density was obtained as 38° by shear tests. Nails used were the tor steel bars of diameter 10 and 12 mm of lengths 1.5 and 1.6 m. The yield strength of tor steel bars was 4.15×10^5 kPa. The configuration of nails was as shown in Fig. 7a, b.

5.3 Facing

In actual soil nailed cuts, where the soil can stand unsupported for excavation depth of about 0.5–1.0 m, a shotcrete or precast panel facing is commonly used. Since dry sand was used in these tests, a vertical excavation face could only be maintained using facing. A 19 mm thick ply board (2.0 m high and 1.0 m wide) was used as a pre-placed continuous facing. Circular holes of respective diameters were made to accommodate the nails of 10 or 12 mm diameter on pre-placed facing at the horizontal and vertical spacings as shown in Fig. 7a, b. The inner periphery of these holes was made smooth by

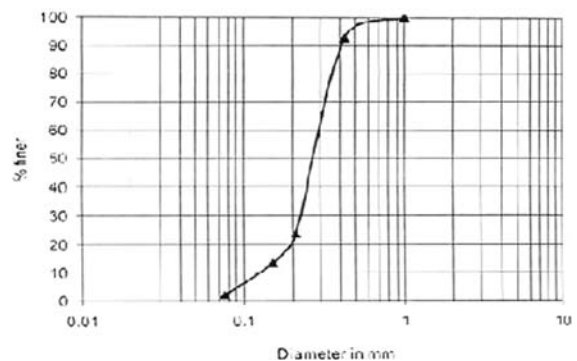


Fig. 6 Particle size distribution curve for sand used in experimental programme (Solani Sand)

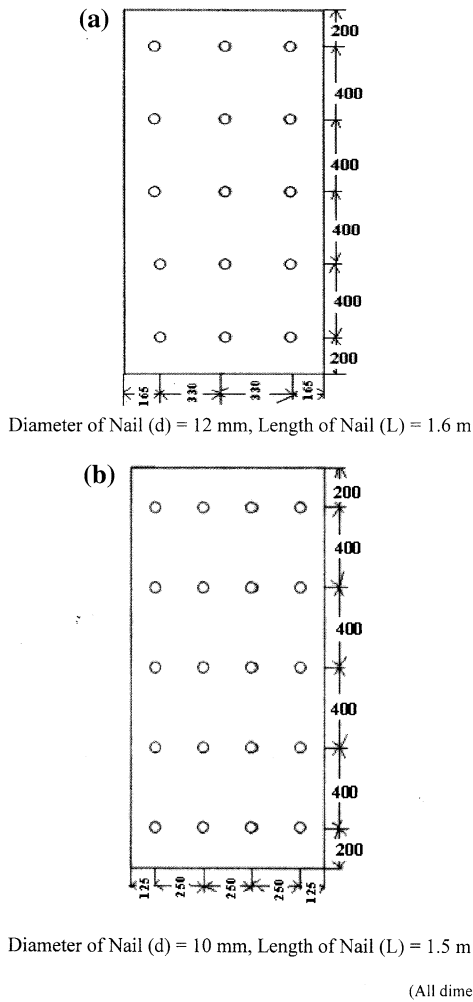


Fig. 7 Horizontal and vertical spacing of nails in model tests

grinding to avoid any friction of the wall material with nail. To avoid the leakage of sand through these holes, flaps of size 25 mm × 25 mm made of 2 mm thick aluminium sheets were fitted on these holes with single rivet to cover these holes. The advantage of these flaps was that it could be turned up and down along the rivet.

The details of test setup are shown in Fig. 8a.

5.4 Test procedure

The following procedure was adopted for construction of nailed cut for model tests:

1. Ply board facing was placed vertically across the tank at 2.5 m from rear end of tank. The facing was brought to absolute vertical position with the

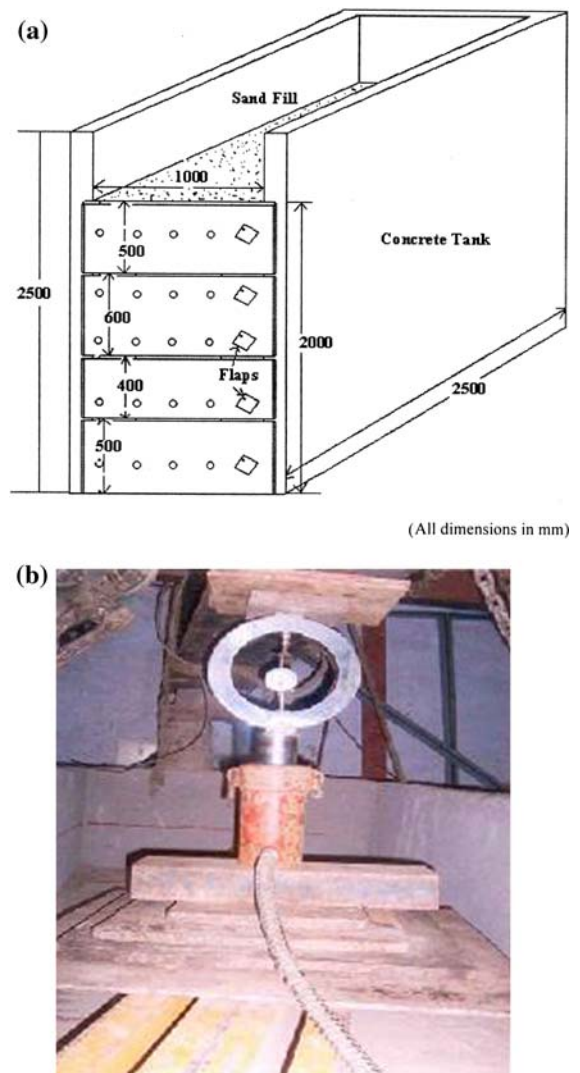


Fig. 8 a Details of model tests set up. b Details of model tests set up

- help of a tri-square and it was clamped at the top of its both ends to restrict the lateral movement of facing during filling of tank.
2. The narrow gaps between the facing and the tank sides were closed by a polyethylene sheet strip bent into an angle along the length.
3. The filling of the sand was done by rainfall technique to achieve the unit weight of sand as 16.5 kN/m³. It corresponds to relative density of sand equal to 70%. To check the density achieved by rainfall technique, a container of known volume (i.e., 0.001 m³) was placed at different depths in tank. By measuring the actual weight of

the sand filled in the containers, unit weight of fill at the respective points was calculated. Average density achieved was observed to be 16.5 kN/m^3 , variation in the density found by rainfall technique at the different depths in the two model tests 1 and 2 was only 5%. While filling the tank, aluminium flaps fixed on holes on front side of the facing were covering all the holes. The sand was filled in tank upto the centre of holes of respective row of nails (upto 200 mm from the bottom of the tank for 1st row of nails).

4. The top surface of sand was leveled properly and the predetermined numbers of nails were placed in the holes at specified horizontal spacing. Total length of the nail was kept as 1,600 mm. One end of the nail was threaded and a circular MS washer of 25 mm outside diameter and 2 mm thickness (with central circular hole of 12 mm diameter) was put on each nail from its threaded end and nail was tightened against the facing with the help of nut.
5. Again sand was filled over these nails in the tank, till the next locations of nails (i.e., at 600, 1,000, 1,400, and 1,800 mm from bottom of the tank). In this way the total depth of nailed backfill was attained behind nailed facing.

5.5 Surcharge Application on Nails Backfill

A rigid steel plate of size 0.8 m width, 2.4 m length, and 25 mm in thickness (density = 100 kN/m^3) was placed centrally on the nailed backfill. Above this steel plate, other steel plates of sizes $1.5 \text{ m} \times 0.8 \text{ m} \times 25 \text{ mm}$ thick, $0.75 \text{ m} \times 0.75 \text{ m} \times 25 \text{ mm}$ thick, and $0.3 \text{ m} \times 0.3 \text{ m} \times 25 \text{ mm}$ thick were placed one above the other. At the centre of the top most steel plate, a proving ring of 300 kN capacity was placed to measure the surcharge applied by hydraulic jack of 500 kN capacity (Fig. 8b). The steel plates were kept on the sand fill to ensure uniform application of surcharge. Surcharge was applied in the increment of 10 kN and the readings for the lateral movement of the facing were taken at the top of excavation for each increment. The process was repeated till failure occurred. For the observed failure surcharge load, the factor of safety of the model nail wall was calculated for the designed length, diameter and spacing of nails considering the side wall friction of

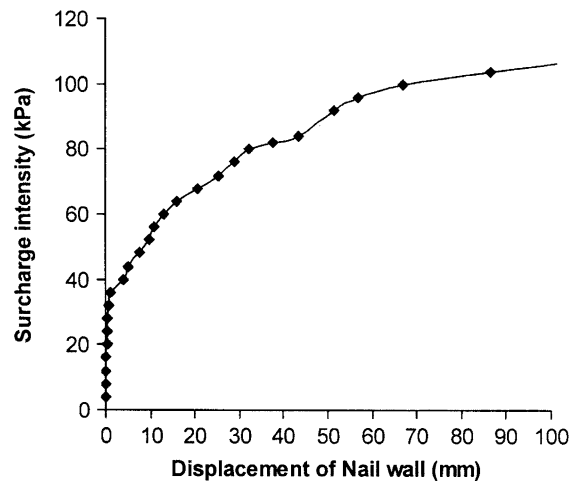


Fig. 9 Surcharge intensity versus displacement of nailed wall for model test 1 ($S_v = 0.4 \text{ m}$, $S_h = 0.33 \text{ m}$, $H = 2 \text{ m}$, $D = 12 \text{ mm}$ and $L/H = 0.8$)

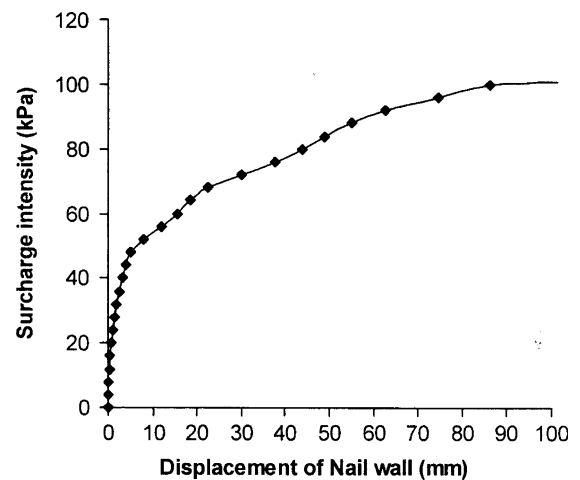


Fig. 10 Surcharge intensity versus displacement of nailed wall for model test 2 ($S_v = 0.4 \text{ m}$, $S_h = 0.25 \text{ m}$, $H = 2 \text{ m}$, $D = 10 \text{ mm}$ and $L/H = 0.75$)

the model tank into account. It may be noted that the value of f^* was obtained for each nail separately by performing pull-out tests at different surcharge intensities. The value of f^* equal to 0.5 was obtained from these tests (Gosavi 2006).

5.6 Test Results

Surcharge intensity versus displacement of the nail wall at top, plots for model tests 1 and 2 are presented in Figs. 9 and 10. From these plots, it was observed

that when the surcharge intensities approached 112.7 kN/m² (test no. 1) and 101.7 kN/m² (test no. 2), excavation failed. The factor of safety of these cuts were obtained for three cases, namely (1) $q = 0$ and (2) $q = 112.7$ and 107 kN/m² in tests no. 1 and 2, respectively. The factors of safety for $q = 0$ case for model tests no. 1 and 2 was worked out as 1.97 and 1.89, respectively. In test no. 1, the factor of safety for $q = 112.7$ kN/m² reduces to 1.01, while in test no. 2 for $q = 101.7$ kN/m², it becomes 0.95. At the verge of failure, the FOS should be unity. The factors of safety computed for the two model tests are 1.01 and 0.95, which are very close to unity.

6 Conclusion

The theoretical analysis has been developed for the design of nailed open inclined excavations, using either driven or grouted nails. The analysis has been supported with the findings of model tests.

Acknowledgments Authors wish to thank Council of Scientific and Industrial Research (CSIR), New Delhi, India, for providing financial support for undertaking this research work.

References

- Chen WF (1975) Limit analysis and soil plasticity, Development in Geotechnical Engineering, vol 7, Elsevier Scientific Publishing Company
- Gässler G, Gudehus G (1981) Soil nailing—some aspects of new technique. In: Proceeding of Xth ICSMFE, Stockholm, vol 3, pp 665–670
- Gässler G, Gudehus G (1983) Soil nailing statistical design. In: Proceeding of VIIIth ECSMFE, Helsinki, vol 2, pp 491–494
- Gosavi M (2006) Behaviour of nailed open cuts, Ph.D. Thesis, Indian Institute of Technology, Roorkee, India
- Gosavi M, Saran S, Mittal S (2006) Software development for design of nailed open cuts, Souvenir of Indo-Australian Conference on Information Technology in Civil Engineering, IIT, Roorkee, India, pp 101–106
- Gupta RP (2003) A study on soil nailing with respect to open excavations and slopes, M.Tech Thesis, Indian Institute of Technology, Roorkee
- Jewell RA (1989) Theory of reinforce wall: revised design charts for steep reinforce slopes. In: Proceedings of the Conference on Reinforced Embankments, Theory and Practice in the British Isles, Cambridge University, pp 1–30
- Jewell RA, Pedley MJ (1990) Soil nailing design: the role of bending stiffness, Ground Engineering, 30–36
- Juran I, Elias V (1992) Ground anchors and soil nails in retaining structures In: Foundation Engineering Handbook, 2nd edn. Van Nostrand Company, pp 868–905
- Juran I, Baudrand G, Khalid F, Elias V (1988) Kinematical limit analysis approach for the design of nailed soil retaining structures. In: International Geotechnical Symposium on Theory and Practice of Earth Reinforcement, Fukuoka, Japan, Balkema, pp 301–305
- Juran I, Baudrand G, Khalid F, Elias V (1990) Kinematic limit analysis for design of soil nailed structures. J Geotech Eng 116(1):54–72. doi:10.1061/(ASCE)0733-9410(1990)116:1(54)
- Mizuno E, Chen WF (1984) Plasticity models for seismic analysis of slopes, Int J Soil Dynamics and Earthquake Engg, 2–7
- Patra CR, Basudhar PK (2001) Nailed soil structure: an overview. Indian Geotech J 31(4):322–362
- Plumelle C, Schlosser C (1990) A French National Research Project on soil nailing: Clouterre, performance of reinforced soil structures. In: Proceedings of International Reinforced Soil Conference, Glasgow, pp 219–223
- Raju GVR (1996) Behaviour of nailed soil retaining structures, Ph.D. Thesis, Nanyang Technological University, Singapore
- Sabhahit N, Madhav MR, Basudhar PK (1996) Seismic analysis of nailed soil slopes—a pseudo-dynamic approach, Earth Reinforcement, Balkema, pp 821–824
- Saha S, Murthy BR, Vatsala AS (2002) Soil nailed walls under dynamic loads, 12th Symposium on Earthquake Engineering, Indian Institute of Technology, Roorkee, pp 434–441
- Saran S, Mittal S, Gosavi M (2005) Pseudo static analysis of nailed vertical excavations in sands. Indian Geotech J 35(4):401–417
- Schlosser F (1982) Behaviour and design of soil nailing. In: Symposium on Recent Developments in Ground Improvement techniques, Bangkok, pp 399–413
- Shen CK, Bang S, Romstad KM, Kulchin L, Denatale JS (1981) Field measurements of an earth support system. ASCE J Getotechnical Eng 107(GT12):1625–1642